Influence of Particle Composition on Remote Sensing Reflectance and MERIS Maximum Chlorophyll Index Algorithm: Examples From Taihu Lake and Chaohu Lake

Lin Qi, Chuanmin Hu, Hongtao Duan, Yuchao Zhang, and Ronghua Ma

***Abstract*—Using data collected from two eutrophic lakes located in eastern China (Taihu Lake, 2330 km^2 and Chaohu Lake, 760 km^2), the influence of variable particle composition on remote sensing reflectance (Rrs, in sr^{-1}) properties and on the Medium Resolution Imaging Spectrometer (MERIS) maximum chlorophyll index (MCI) algorithm for estimating near-surface chlorophyll-a concentrations (Chla, in $\mu g \cdot L^{-1}$) is demonstrated. Although separated by a distance of only ~200 km, the two lakes showed dramatic differences in particle composition, with Taihu Lake dominated by inorganic particles and Chaohu Lake dominated by organic particles. Such differences led to variable Rrs spectral slopes in the red and near-IR bands and perturbations to the MCI algorithm. A modified MCI algorithm (MCIT) was then developed to reduce the impact of turbidity caused by inorganic particles. Root-mean-square errors in Chla retrievals decreased from 129.5% to 43.5% when using this new approach compared with the MCI algorithm in Taihu Lake for Chla ranging between ~5 and 100 $\mu g \cdot L^{-1}$. Application of this approach to other turbid water bodies, on the other hand, requires validation and possibly further tuning.**

***Index Terms*—Apparent optical properties (AOPs), Chaohu Lake, chlorophyll a (Chla), fluorescence line height (FLH), maximum chlorophyll index (MCI), Medium Resolution Imaging Spectrometer (MERIS), Moderate Resolution Imaging Spectroradiometer (MODIS), particle composition, remote sensing reflectance (Rrs), Taihu Lake.**

Manuscript received October 30, 2014; revised December 12, 2014; accepted December 18, 2014. This work was supported in part by the National Natural Science Foundation of China under Grant 41171271, Grant 41171273, and Grant 41101316, by the National High Technology Research and Development Program of China under Grant 2014AA06A509, and by the 135-Program of the Nanjing Institute of Geography and Limnology, Chinese Academy of Sciences (NIGLAS) under Grant NIGLAS2012135014 and Grant NIGLAS2012135010. *(Corresponding author: R. Ma.)*

L. Qi is with the State Key Laboratory of Lake Science and Environment, Nanjing Institute of Geography and Limnology, Chinese Academy of Sciences, Nanjing 210008, China; with the College of Marine Science, University of South Florida, St. Petersburg, FL 33701 USA; and also with the University of Chinese Academy of Sciences, Beijing 100864, China.

C. Hu is with the College of Marine Science, University of South Florida, St. Petersburg, FL 33701 USA.

H. Duan, Y. Zhang, and R. Ma are with the State Key Laboratory of Lake Science and Environment, Nanjing Institute of Geography and Limnology, Chinese Academy of Sciences, Nanjing 210008, China (e-mail: rhma@niglas.ac.cn).

Color versions of one or more of the figures in this paper are available online at http://ieeexplore.ieee.org.

Digital Object Identifier 10.1109/LGRS.2014.2385800

I. Introduction

BOTH inherent and apparent optical properties (IOPs and AOPs) in aquatic environments are affected by variable concentrations and compositions of particulate materials (e.g., [2], [23], [25], [27], and [30]), which in turn determine the design of remote sensing inversion algorithms. One such example is the maximum chlorophyll index (MCI) algorithm, which was designed for the Medium Resolution Imaging Spectrometer (MERIS) to estimate chlorophyll-a concentrations (Chla, in $\mu g \cdot L^{-1}$) in highly productive waters [11].

Similar to the fluorescence line height (FLH) algorithm [18] designed for MODIS, MCI is a measure of the reflectance (or the total radiance or the water-leaving radiance) height at 709 nm referenced against a linear baseline formed between two neighboring wavelengths (681 and 754 nm). Recent advancement in this type of algorithm led to a maximum peak height (MPH) algorithm that adapts to the slight wavelength shift in the reflectance peak [20], which works similar to the MCI for eutrophic lakes. MCI has been used to map intense phytoplankton blooms in coastal waters and macroalgae (e.g., *Sargassum spp.*) distributions in the Gulf of Mexico and the Atlantic Ocean [12] and [13].

However, radiative transfer simulations have shown that such an approach would be susceptible to interference by inorganic particles (i.e., minerals or suspended sediments) as these particles would falsely lead to increases in the FLH signal [9], [21]. Based on the same arguments as in these pioneering studies, MCI would be also expected to suffer from similar perturbations. Reference [9] demonstrated the impact of sediments on the FLH–Chla relationship using limited field data, yet to our best knowledge, there has been no report to show similar impact on the MCI–Chla relationship. Furthermore, although Gilerson *et al.* [10] proposed a preliminary solution to minimize the impact of sediments, the solution relies on accurate estimates of the in-water IOPs to form the elastic component in the reflectance spectrum. Such estimates are often problematic for turbid coastal or inland waters due to uncertainties in the atmospheric correction of satellite data and the water's optical complexity in affecting IOP retrieval algorithms.

Here, using data collected from two adjacent lakes in eastern China, i.e., Taihu Lake (2300 km^2) and Chaohu Lake (760 km^2), we show the influence of variable particle composition on spectral reflectance and on the MERIS MCI algorithm performance. An empirical correction to the original MCI algorithm is developed and validated with MERIS data for

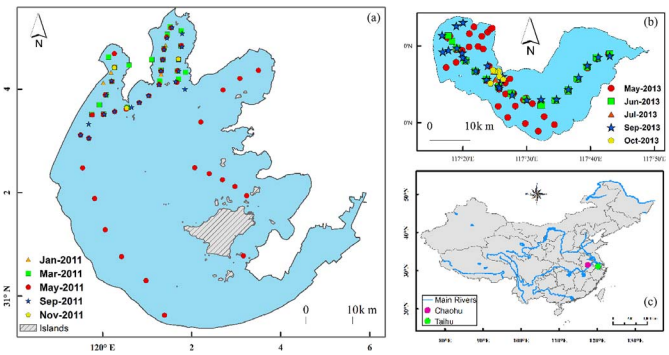

Fig. 1. Maps showing the sample locations in (a) Taihu Lake and (b) Chaohu Lake, which are both located in (c) China. Field stations for various sampling dates are annotated with different colors.

Taihu Lake, where the proportion of inorganic particles to total suspended matter (TSM) is significantly higher than that of Chaohu Lake.

II. Data and Methods

Both Taihu Lake and Chaohu Lake are located in eastern China, along the Yangtze River delta (see Fig. 1), with their surfaces areas being $\sim$2300 km^2 and 760 km^2, respectively. The biooptical properties and long-term algal bloom trends in Taihu Lake have been well documented (e.g., [6], [14], and [25]). In contrast, although biooptical properties and field-based algorithms have been reported for Chaohu Lake (see [4], [26], and [28]), long-term trends in bloom dynamics based on satellite data have not been reported for this area.

A. Field Data

A series of cruise surveys was conducted to study the biooptical properties and particle compositions in the two lakes. In total, 105 and 132 stations were measured from 5 surveys of Taihu and 5 surveys of Chaohu between January 2011 and November 2011 and between May 2013 and October 2013, respectively (see Fig. 1). At each station, the remote sensing reflectance (Rrs) data were collected and processed with an Analytical Spectral Devices Inc., handheld spectrometer following the NASA Ocean Optics protocols [22]. Immediately following the Rrs measurement, water samples were collected at the surface ($\sim$30 cm) with a 2-L polyethylene bucket. Water samples were filtered onboard and then returned to the laboratory to determine Chla and particle composition on the same day using 47-mm Whatman GF/F glass fiber filters and ethanol extraction [19]. Concentrations of TSM (in mg $\cdot$ L^{-1}) were gravimetrically determined from the samples filtered on precombusted (957 °C overnight) and preweighed filters. TSM was further differentiated into inorganic suspended matter (ISM) and organic suspended matter (OSM) by burning the organic matter from the filters at 550 °C for 3 h and weighing the filters again. Table I summarizes the statistics of Chla, TSM, ISM, and OSM measured from the two lakes.

B. MERIS Data

MERIS Level-1B full-resolution (300 m) data were obtained from NASA (http://oceancolor.gsfc.nasa.gov). The data were first processed with several existing software packages (e.g., SeaDAS, BEAM), resulting in unsatisfactory Rrs data products for a number of reasons (e.g., [8]). Thus, an alternative approach was used to correct the atmosphere effects by ozone absorption and Rayleigh scattering. The resulting Rrc (dimensionless) was used to compose the red–green–blue (RGB) images and to derive the Rrc-based MCI and its alternative form.

TABLE I
Statistics of Water Quality Parameters Determined From Taihu Lake and Chaohu Lake

	Taihu Lake		Chaohu Lake	
	Mean±Std	Min – Max	Mean±Std	Min – Max
Chla (μg/L)	18.3±25.3	0.5-222.6	88.3±204.4	3.0-1538.3
TSM (mg/L)	35.4±22.2	9.4-150.6	60.9±57.4	10.0-394.0
ISM (mg/L)	27.0±20.1	4.2-132.5	26.6±16.4	2.0-94.0
OSM (mg/L)	8.4±5.6	3.1-41.1	35.0±50.9	0.0-358.0

In all calculations, MCI was derived as

$$\mathrm{MCI} = R_{\lambda 2} - [R_{\lambda 1} + (R_{\lambda 3} - R_{\lambda 1}) * (\lambda_2 - \lambda_1)/(\lambda_3 - \lambda_1)]. \quad (1)$$

Here, $\lambda_1 = 665$ nm, $\lambda_2 = 709$ nm, and $\lambda_3 = 754$ nm. R represents either Rrs or Rrc, where the field hyperspectral data were averaged over the MERIS bandwidths.

For algorithm vaidation, due to the relatively narrow swath (1150 km) of MERIS and turbid atmosphere, as well as frequent sun glint, it was difficult to find strictly concurrent (e.g., ± 3 h) field and MERIS measurements. The time window was therefore relaxed to ± 48 h. Standard statistics such as root-mean-square error (RMSE) and coefficient of determination (R^2) were used to gauge the accuracy of the MERIS-derived Chla.

III. Results

A. Influence of Particle Composition on Rrs and MCI

Fig. 2 shows the field-measured Rrs and particle concentrations and compositions from Taihu and Chaohu, from which several observations can be made.

First, although the general shapes of the Rrs from the two lakes appear similar, reflecting typical eutrophic waters (e.g., local peaks around 560 and 700 nm, and local trough around 670 nm), the Rrs magnitudes of Chaohu are significantly higher (mean Rrs560 $= 0.04$ sr^{-1} and mean Rrs710 $= 0.032$ sr^{-1} versus 0.025 sr^{-1} and 0.018 sr^{-1} for Taihu Lake), apparently due to their different TSM distributions. Some spectra show high Rrs values between 750 and 900 nm, which is a possible result of floating algae and/or Rrs data processing residual errors. However, they appear to be spectrally related and thus would not impact the band-subtraction algorithms in the following. Although both lakes showed large ranges (10 to $>$150 mg $\cdot$ L^{-1}), the mean TSM in Chaohu (61.0 ± 57.0 mg $\cdot$ L^{-1}) was significantly higher than that in Taihu (35.4 ± 22.2 mg $\cdot$ L^{-1}) [see Fig. 2(c) and (d)]. Half of the Taihu samples had TSM < 29.5 mg $\cdot$ L^{-1}, while half of the Chaihu samples had TSM > 44.0 mg $\cdot$ L^{-1}. Rrs generally increases with TSM in the green–red spectral region, thus explaining the observed Rrs differences between the two lakes.

The two lakes not only differ in their TSM but also in their variable contributions of ISM and OSM. Fig. 2(e) and (f) shows that TSM in Taihu Lake was dominated by ISM,

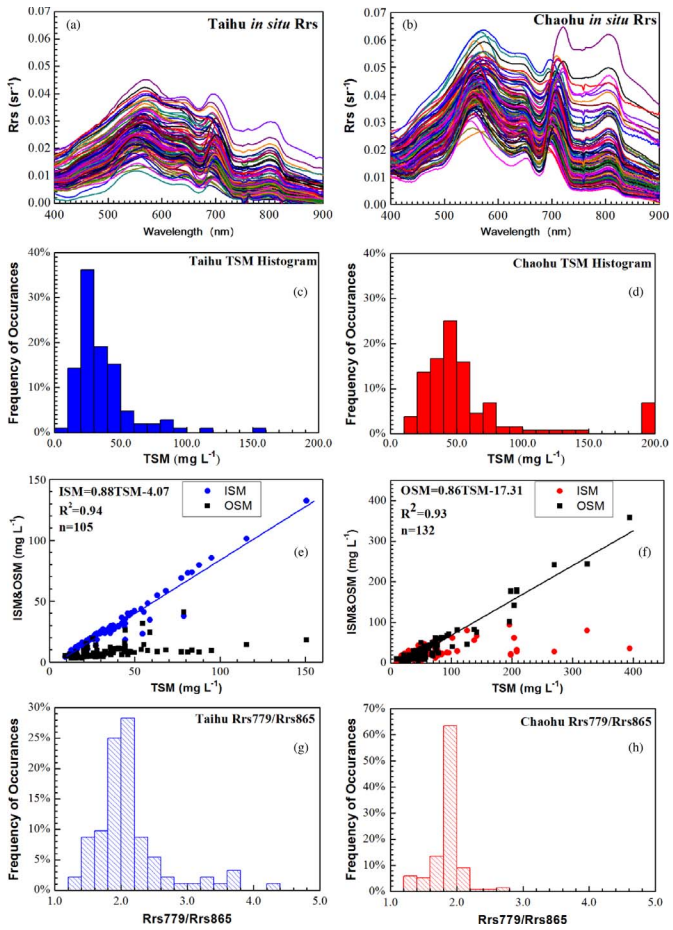

Fig. 2. Field-measured reflectance and particle properties for (a), (c), (e), and (g) Taihu Lake and (b), (d), (f), and (h) Chaohu Lake. Rrs: remote sensing reflectance (in sr^{-1}); TSM: total suspended matter (in $mg \cdot L^{-1}$); ISM: inorganic suspended matter (in $mg \cdot L^{-1}$); OSM: organic suspended matter (in $mg \cdot L^{-1}$).

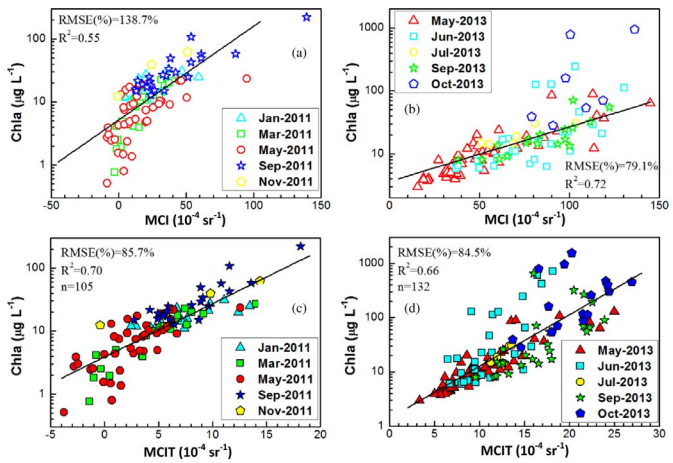

Fig. 3. Relationships between field-measured Chla and Rrs-derived (a) and (b) MCI and (c) and (d) MCIT for (left column) Taihu Lake and (right column) Chaohu Lake.

whereas that in Chaohu Lake was dominated by OSM. On average, OSM in Taihu Lake was only 26% ± 13% of TSM, as compared with 49% ± 22% in Chaohu Lake. Although particle size and particle refraction index were not measured, inorganic particles generally exhibit smaller size ranges (e.g., 1–10 μm) and higher refraction indexes than organic particles (e.g., 2–20 μm for nanophytoplankton and 20–200 μm for

TABLE II
STATISTICAL SUMMARY OF THE ALGORITHM PERFORMANCE OF THE MCI, THE MCIT, AND THE RRS709/RRS665 BAND RATIO APPROACHES FOR CHLA (IN MICROGRAMS PER LITER) RETRIEVALS

Chla Range	Method	Taihu Lake			Chaohu Lake		
		N	R^2	RMSE (%)	N	R^2	RMSE (%)
0.5<Chla<=1600 (All Data)	MCI	105	0.55	138.7%	132	0.72	79.1%
	MCIT	105	0.70	85.4%	132	0.66	84.5%
	Rrs709/Rrs665	105	0.55	148.4	132	0.70	84.4
5<Chla<=100	MCI	78	0.41	47.1	98	0.71	45.8
	MCIT	78	0.58	34.5	98	0.67	44.9
	Rrs709/Rrs665	78	0.59	39.1	98	0.68	44.8

microphytoplankton), leading to higher spectral backscattering (b_b) slopes [5]). Furthermore, for the same particle concentrations, inorganic particles tend to have higher backscattering efficiency and higher reflectance in the red [23]. Because for the NIR wavelengths Rrs is approximately proportional to b_b/a, and absorption by color-dissolved organic matter and phytoplankton pigments is small and by other particles is spectrally flat [1], Rrs in the NIR is also expected to have a higher spectral slope for the ISM-rich Taihu Lake than for the OSM-rich Chaohu Lake. Such a speculation is confirmed by the Rrs(779)/Rrs(865) ratios from the two lakes [see Fig. 2(g) and (h)]. The mean ratio for Taihu Lake is 2.14 ± 2.69, with half of the points > 4.73. In contrast, the mean ratio for Chaohu Lake is 1.85 ± 2.08, with >88% of the points < 2.0.

The influence of particle composition on the relationships between MCI (Rrs) and Chla was also examined [see Fig. 3(a) and (b)]. The relationship for Taihu Lake was weaker than for Chaohu Lake, with a lower R^2 and a higher RMSE between the measured Chla and the best fit line. Indeed, a tighter relationship between MCI and Chla was observed (RMSE = 42.4%) for Chaohu Lake when MCI was $< 80 \times 10^{-4}$ [see Fig. 3(b)], suggesting that Chla in this range could be estimated from MCI fairly accurately. For MCI $> 80 \times 10^{-4}$, the data for Chaohu were highly scattered, which is possibly due to increased patchiness (scums) in high-Chla waters. Such patchiness made it difficult to measure the Rrs and collect samples from the same water. Nevertheless, Fig. 3(b) indicates that MCI may be used as a relatively reliable index to estimate Chla for Chaohu.

Such fidelity degraded for Taihu Lake [see Fig. 3(a)]. Not only was R^2 much lower but also RMSE was significantly higher than for Chaohu Lake. There was also more data scatter below the best fit line than above the fitted line. For the same Chla, the points below the best fit line represent those with higher MCI values. This phenomenon, i.e., sediment-induced false "fluorescence" values, was well studied in [9] and [21]. Even after excluding Chla < 5 and > 100 μg/L, some of the data scatter still remained, although RMSE decreased significantly (see Table II). It is speculated that such data scatter was due to the dominance of ISM in Taihu Lake, requiring algorithm modifications.

B. Modified MCI to Partially Remove Impact of ISM

Thus, a modified MCI was developed as

$$\text{MCIT} = \text{MCI}/(1 + 0.1 \times (R_{\lambda 3} - R_{\lambda 4})),$$
$$\lambda_3 = 754 \text{ nm}, \ \lambda_4 = 865 \text{ nm} \quad (2)$$

where "T" in MCIT represents turbidity. The rationale of using a two-band subtraction term in the denominator to represent

TSM was demonstrated in [7]. Basically, R in the NIR is a monotonic function of TSM, and subtraction of R at a longer wavelength is to account for aerosol perturbations. Compared with other popular approaches, the $(R_{\lambda 3} - R_{\lambda 4})$ approach showed better relationship with TSM (see [7, Fig. 4]), which is thus adopted here as a TSM index in (2). The design of the mathematical form in (2) was to lower MCI when TSM was high $((R_{\lambda 3} - R_{\lambda 4}) > 0.0)$ while keeping it the same when TSM was low $((R_{\lambda 3} - R_{\lambda 4}) \sim 0.0)$. The coefficients in (2) were then determined through empirical regression. Fig. 3(c) and (d) shows the relationship between MCIT and Chla for Taihu Lake and Chaohu Lake, respectively. Compared with Fig. 3(a), the MCIT–Chla relationship for Taihu Lake exhibits less scatter than the MCI–Chla relationship, with an increased R^2 and a decreased RMSE. In particular, many of the points below the original MCI–Cha best fit line are now closer to the fitted line, indicating reduced impact of TSM on the retrieval. In contrast, the same MCI modification for Chaohu did not lead to improvement in the MCI–Chla relationship but instead made it slightly worse [see Fig. 3(d), Table II]. Such a result also confirms that the MCI–Chla relationship is influenced more by ISM than by OSM. For this reason, MCIT may be used for Taihu, but MCI should be used for Chaohu.

C. Application of Modified MCI to MERIS Data

In order to apply the Rrs-based MCI and MCIT algorithms to MERIS Rrc data, the effects from variable aerosols must first be considered. This was achieved through simulations by adding variable aerosol properties (extracted from SeaDAS LUTs) to the field Rrs under various observing scenarios (e.g., see [24]). The simulations led to new regression coefficients with field-measured Chla as follows:

$$\text{Chla}_{\text{MCI}} = 4.06 * \exp(0.025 * \text{MCI}_{\text{Rrc}}) \quad (3)$$

$$\text{Chla}_{\text{MCIT}} = 3.77 * \exp(0.350 * \text{MCIT}_{\text{Rrc}}). \quad (4)$$

Fig. 4 shows four MERIS scenes for Taihu with different TSM perturbations. To facilitate a visual comparison, the near-concurrent (±48 h) field-measured Chla were annotated and color coded in the same way as the underlying MERIS images. For the two sediment-rich cases [see Fig. 4(a)–(f)], the MCIT algorithm suppressed the derived Chla for most of the lake waters, leading to improved Chla retrievals as most of the falsely elevated MERIS Chla in Fig. 4(b) and (e) were reduced to reasonable levels in Fig. 4(c) and (f). For the two sediment-poor cases [see Fig. 4(g)–(l)], the MCIT resulted in similar Chla patterns as the MCI, indicating that the effect of the MCIT is mostly on sediment-rich waters as it was designed.

The visual inspection was reinforced by the validation statistics in Fig. 4(m). The MCIT led to significantly improved Chla retrievals over the MCI ($n = 42$), as shown by the much reduced RMSE (from 129.5% to 43.5%). Most of the improvement came from the sediment-rich points that were overestimated by the MCI algorithm.

IV. Discussion

While the exact reason why the two adjacent lakes have dramatic differences in their particle compositions is unclear, it is speculated that the shallower water depth of Taihu (mean = 1.9 m, max = 2.6 m) than Chaohu (mean = 2.5 m, max = 5.0 m) makes the bottom sediments (mostly inorganic) more susceptible to wind mixing. Another possible reason is that Taihu Lake receives inputs from > 200 rivers, which may carry a significant amount of inorganic particles due to the rapid industrialization and economic growth. In contrast, Chaohu Lake's drainage region is relatively less developed, with only ∼30 rivers discharging to the lake.

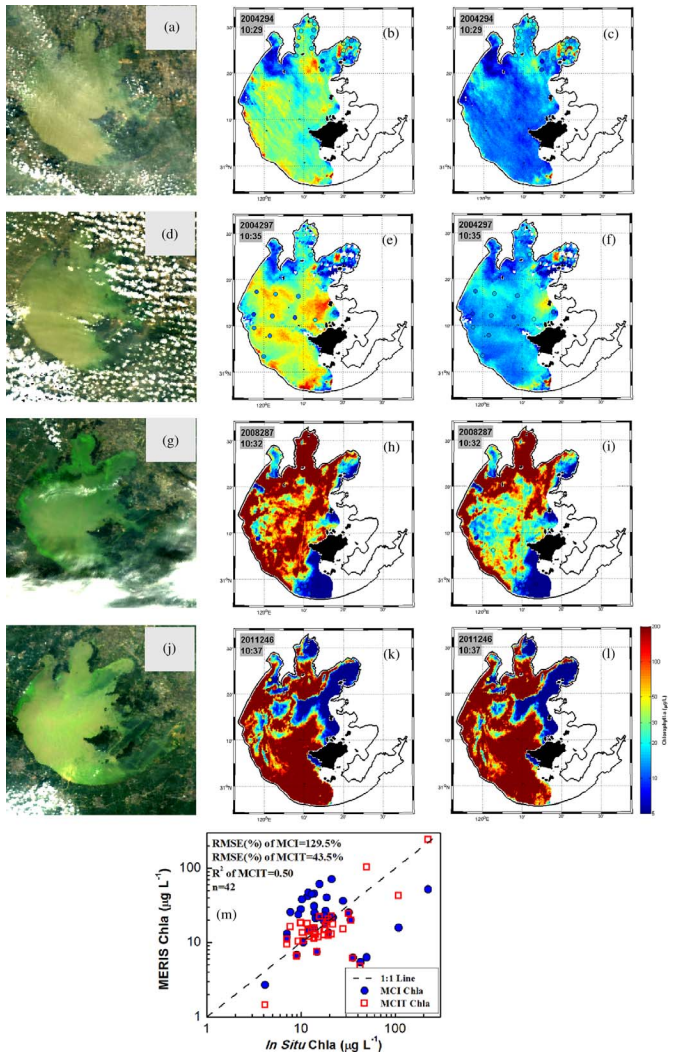

Fig. 4. MERIS data collected in Taihu Lake on (a)–(c) October 20, 2004, (d)–(f) October 23, 2004, (g)–(i) October 13, 2008, and (j)–(l) September 3, 2011. (Left column) RGB images where sediment resuspension (yellowish color) and dense bloom (light green) can be visualized. (Middle column) MCI-derived Chla (in micrograms per liter) distributions. (Right column) MCIT-derived Chla (in micrograms per liter) distributions. For comparison, the field-measured Chla within ±48 h are annotated on the Chla images using the same color legend and are used to evaluate the (m) MERIS-derived Chla using both the MCI and the MCIT algorithms.

The differences in the two lakes' inorganic/organic particle compositions apparently led to different Rrs779/Rrs865 ratios, which would impact atmospheric correction performance [16]. Furthermore, in turbid waters nonalgal constituents often significantly contribute to the reflectance in the blue–green bands, making it more appropriate to use red and NIR bands for Chla retrievals (see reviews in [3] and [15]).

However, regression between field-measured NIR/red Rrs ratios and Chla generally did not show improved performance over MCI (see Table II), suggesting that MCI would be a

better choice than NIR/red once the effect of ISM perturbations is reduced through the use of MCIT (Figs. 3 and 4). The limited dataset, on the other hand, suggests that additional validation is required once more field data are available. Likewise, application of the newly developed MCIT approach to other lakes also requires further algorithm tuning and validation. Ideally the choice of whether to use MCIT or MCI may be determined at pixel level using Rrs ratios [see Fig. 2(g) and (h)], yet in practice, this is currently difficult due to atmospheric correction uncertainties. Nevertheless, once *a priori* knowledge of the particle composition is available, such a choice can be made, and application of MCIT may improve the overall algorithm performance [see Figs. 3(a) and (c) and 4]. Given the fact that MERIS has stopped functioning since April 2012, future satellite sensors with the 709-nm or similar bands may be used in conjunction with field surveys to further develop locally tuned MCIT-like algorithms to improve Chla retrievals for turbid lakes and coastal/estuarine waters.

V. Conclusion

This letter has demonstrated how two adjacent eutrophic lakes in eastern China with different particle loads and compositions exhibit variable AOPs in the form of Rrs. Correspondingly, the MERIS Chla retrieval algorithm based on the red and NIR bands performed differently for the two lakes. The empirical adjustment developed here for the retrieval algorithm that takes into account high inorganic particle loads may serve as an intermediate solution toward the ultimate goal of establishing long-term Chla data records for turbid inland lakes covering the entire dynamic range under all possible scenarios.

Acknowledgment

The authors would like to thank the two anonymous reviewers who provided valuable comments to help improve the manuscript.

References

[1] M. Babin and D. Stramski, "Light absorption by aquatic particles in the near-infrared spectral region," *Limnol. Oceanogr.*, vol. 47, pp. 911–915, 2002.

[2] C. E. Binding, D. G. Bowers, and E. G. Mitchelson-Jacob, "Estimating suspended sediment concentrations from ocean colour measurements in moderately turbid waters; the impact of variable particle scattering properties," *Remote Sens. Environ.*, vol. 94, no. 3, pp. 373–383, Feb. 2005.

[3] D. Blondeau-Patissier, J. F. R. Gower, A. G. Dekker, S. R. Phinn, and V. E. Brando, "A review of ocean color remote sensing methods and statistical techniques for the detection, mapping and analysis of phytoplankton blooms in coastal and open oceans," *Progr. Oceanogr.*, vol. 123, pp. 123–144, Apr. 2014.

[4] Y. Dai, S. Li, and X. Wang, "Measurement of analysis on the apparent optical properties of water in Chaohu Lake," *China Environ. Sci.*, vol. 28, pp. 979–983, 2008.

[5] D. Doxaran, M. Babin, and E. Leymarie, "Near-infrared light scattering by particles in coastal waters," *Opt. Exp.*, vol. 15, no. 20, pp. 12 834–12 849, Oct. 2007.

[6] H. Duan *et al.*, "Two-decade reconstruction of algal blooms in China's Lake Taihu," *Environ. Sci. Technol.*, vol. 43, no. 10, pp. 3522–3528, May 2009.

[7] L. Feng, C. Hu, X. Chen, L. Tian, and L. Chen, "Human induced turbidity changes in Poyang Lake between 2000 and 2010: Observations from MODIS," *J. Geophys. Res.*, vol. 117, no. C7, Jul. 2012, Art. ID. C07006.

[8] L. Feng, C. Hu, X. Han, X. Chen, and L. Qi, "Long-term distribution patterns of chlorophyll-a concentration in China's largest freshwater lake: MERIS full-resolution observations with a practical approach," *Remote Sens.*, vol. 7, no. 1, pp. 275–299, Dec. 2014.

[9] A. Gilerson *et al.*, "Fluorescence component in the reflectance spectra from coastal waters. Dependence on water composition," *Opt. Exp.*, vol. 15, no. 24, pp. 15702–15721, Nov. 2007.

[10] A. Gilerson *et al.*, "Fluorescence component in the reflectance spectra from coastal waters. II. Performance of retrieval algorithms," *Opt. Exp.*, vol. 16, no. 4, pp. 2446–2460, Feb. 2008.

[11] J. Gower, S. King, G. Borstad, and L. Brown, "Detection of intense plankton blooms using the 709 nm band of the MERIS imaging spectrometer," *Int. J. Remote Sens.*, vol. 26, pp. 2005–2012, 2005.

[12] J. Gower, C. Hu, G. Borstad, and S. King, "Ocean color satellites show extensive lines of floating Sargassum in the Gulf of Mexico," *IEEE Trans Geosci. Remote Sens.*, vol. 44, no. 12, pp. 3619–3625, Dec. 2006.

[13] J. Gower, S. King, and P. Goncalves, "Global monitoring of plankton blooms using MERIS MCI," *Int. J. Remote Sens.*, vol. 29, no. 21, pp. 6209–6216, 2008.

[14] C. Hu *et al.*, "Moderate resolution imaging spectroradiometer (MODIS) observations of cyanobacteria blooms in Taihu Lake, China," *J. Geophys. Res., Oceans*, (1978–2012), vol. 115, no. C4, 2010, Art. ID. C04002.

[15] C. Hu and J. Campbell, "Oceanic chlorophyll-a content. In Biophysical applications of satellite remote sensing," in *Springer Remote Sensing/ Photogrammetry*, J. M. Hanes Ed. Berlin, Germany: Springer-Verlag, 2014.

[16] L. Jiang and M. Wang, "Improved near-infrared ocean reflectance correction algorithm for satellite ocean color data processing," *Opt. Exp.*, vol. 22, no. 18, pp. 21 657–21 678, Sep. 2014.

[17] C. Le *et al.*, "Evaluation of chlorophyll-a remote sensing algorithms for an optically complex estuary," *Remote Sens. Environ.*, vol. 129, pp. 75–89, Feb. 2013.

[18] R. M. Letelier and M. R. Abbott, "An analysis of chlorophyll fluorescence algorithms for the Moderate Resolution Imaging Spectrometer (MODIS)," *Remote Sens. Environ.*, vol. 58, no. 2, pp. 215–223, Nov. 1996.

[19] R. Ma, J. Tang, and J. Dai, "Bio-optical model with optimal parameter suitable for Taihu Lake in water colour remote sensing," *Int. J. Remote Sens.*, vol. 27, no. 19, pp. 4305–4328, 2006.

[20] M. W. Matthews, S. Bernard, and L. Robertson, "An algorithm for detecting trophic status (chlorophyll-a), cyanobacterial-dominance, surface scums and floating vegetation in inland and coastal waters," *Remote Sens. Environ.*, vol. 124, pp. 637–652, Sep. 2012.

[21] D. McKee, A. Cuningham, D. Wright, and L. Hay, " Potential impacts of nonalgal materials on water-leaving Sun induced chlorophyll fluorescence signals in coastal waters," *Appl. Opt.*, vol. 46, no. 31, pp. 7720–7729, Nov. 2007.

[22] J. L. Mueller *et al.*, Biogeochemical and bio-optical measurements and data analysis protocols: Ocean optics protocols for satellite ocean color sensor validation, National Aeronautical Space administration, Greenbelt, MD, USA, Revision 4, 2, NASA/TM-2003-21621, 2003.

[23] C. Neil, A. Cunningham, and D. McKee, "Relationships between suspended mineral concentrations and red-waveband reflectances in moderately turbid shelf seas," *Remote Sens. Environ.*, vol. 115, no. 12, pp. 3719–3730, Dec. 2011.

[24] L. Qi, C. Hu, H. Duan, J. Cannizzaro, and R. Ma, "A novel MERIS algorithm to derive cyanobacterial phycocyanin pigment concentrations in a eutrophic lake: Theoretical basis and practical considerations," *Remote Sens. Environ.*, vol. 154, pp. 298–317, Nov. 2014.

[25] D. Sun *et al.*, "Light scattering properties and their relation to the biogeochemical composition of turbid productive waters: A case study of Lake Taihu," *Appl. Opt.,* 48, no. 11, pp. 1979–1989, Apr. 2009.

[26] D. Sun *et al.*, "Scattering and backscattering characteristics of Lake Chaohu," *Environ. Sci.*, vol. 31, no. 6, pp. 1428–1434, Jun. 2010, (in Chinese with English abstract).

[27] O. Ulloa, S. Sathyendranath, and T. Platt, " Effect of the particle-size distribution on the backscattering ratio in seawater," *Appl. Opt.*, vol. 33, no. 30, pp. 7070–7077, Oct. 1994.

[28] Q. Wang *et al.*, " Estimation of suspended sediment concentration based on bio-optical mechanism and HJ-1 image in Chaohu Lake," *Sci. China Earth Sci.*, vol. 53, pp. 58–66, 2010.

[29] X. Wen, " Research on the features of chlorophyll-a derived from rapideye and EOS/MODIS data in chaohu lake," in *Proc. IOP Conf. Series, Earth Environ. Sci.*, vol. 17, 2014, Art. ID. 012111.

[30] S. B. Wozniak, D. Stramski, "Modeling the optical properties of mineral particles suspended in seawater and their influence on ocean reflectance and chlorophyll estimation from remote sensing algorithms," *Appl. Opt.*, vol. 43, no. 17, pp. 3489–3503, Jun. 2004.